

Characterization of Alcohol Dehydrogenase from Permeabilized Brewer's Yeast Cells Immobilized on the Derived Attapulgit Nanofibers

Quan Zhao · Yi Hou · Geng-Hao Gong · Ming-An Yu ·
Lan Jiang · Fei Liao

Received: 5 April 2009 / Accepted: 5 June 2009 /
Published online: 4 July 2009
© Humana Press 2009

Abstract Alcohol dehydrogenase (ADH) from permeabilized brewer's yeast was immobilized on derived attapulgit nanofibers via glutaraldehyde covalent binding. The effect of immobilization on ADH activity, optimum temperature and pH, thermal, pH and operational stability, reusability of immobilized ADH, and bioreduction of ethyl 3-oxobutyrate (EOB) to ethyl(S)-3-hydroxybutyrate ((S)-EHB) by the immobilized ADH were investigated. The results show the immobilized ADH retained higher activity over wider ranges of pH and temperature than those of the free. The optimum temperature and pH were 7.5 and 35 °C, respectively, and 58% of the original activity was retained after incubation at 35 °C for 32 h. More importantly, in bioreduction of EOB mediated by immobilized ADH, the conversion of substrate and enantiomeric excess (ee) of product reached 88% and 99.2%, respectively, within 2 h and retained about 42% of the initial activity after eight cycles.

Keywords Alcohol dehydrogenase(ADH) · Ethyl(S)-3-hydroxybutyrate((S)-EHB) · Permeabilized brewer's yeast cells · Immobilization · Attapulgit nano-fibrils

Introduction

Permeabilized cells are promising biocatalysts for the synthesis of optically active alcohols. Specifically, excellent results were observed for the bioreduction of different esters of 3-

Electronic supplementary material The online version of this article (doi:10.1007/s12010-009-8692-y) contains supplementary material, which is available to authorized users.

Q. Zhao · Y. Hou · G.-H. Gong · M.-A. Yu (✉)
College of Pharmaceutical Sciences, Chongqing Medical University, Chongqing 400016, China
e-mail: minganyu666@yahoo.com.cn

L. Jiang
College of Environmental and Biological Engineering,
Chongqing University of Technology and Business, Chongqing 400067, China

F. Liao
Chongqing Key Laboratory of Biochemistry and Molecular Pharmacology,
Chongqing Medical University, Chongqing 400016, China

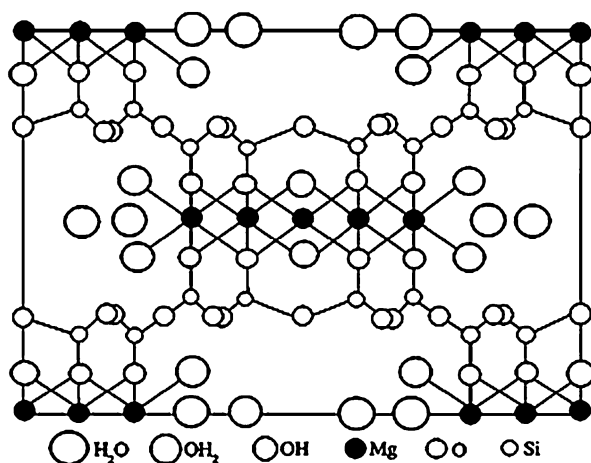
ketobutyric acid [1–4]. However, with permeabilized cells being reused, the activities of the intracellular enzymes and the productivity of chiral alcohol was significantly decreased, respectively [3]. Therefore, through isolation and immobilization techniques, making it into a new biocatalyst having good enzyme stability and higher operational stability is very necessary. From that point of view, the extraction of intracellular alcohol dehydrogenases (ADH) (E.C.1.1.1.1) from permeabilized brewer's yeast has great significance in practicality. Moreover, ADH was routinely applied by companies, e.g., Jülich Chiral Solutions and Wacker Fine Chemicals, for the synthesis of optically active molecules such as alcohols, diols, and hydroxy ester. Processes for the multiton production of different optically active alcohols have recently been established at Wacker Fine Chemicals, Munich [5].

However, enzymes are inherently labile. In order to enhance the properties such as thermal, reusability, storage and operational stability, etc., enzymes must be immobilized by various techniques such as adsorption, covalent binding or binding to a support (carrier), encapsulation or entrapment, and cross-linking of enzymes or combinations thereof. Among these, the covalent binding method is the most effective compared to the other approaches. Firstly, the covalent bond between the enzyme and carrier is strong to keep the enzyme fixed to the carrier under industrial conditions of high reactant and product concentrations and high ionic strength. Furthermore, in comparison with the encapsulation or entrapment of enzymes, the particle size is defined prior to immobilization, and in many cases, the particles are more stable against shear forces [6, 7].

However, in the past, most of the reported processes involving immobilized ADH were based on adsorption and entrapment technique [8]. Only a few examples using covalent binding are described [9, 10]. The support (carrier) used included a synthetic organic polymer, a biopolymer, or an inorganic solid [11–14]. The major problem with polymer supports is lower pH and thermal stabilities, while inorganic supports (carriers) for immobilization are of great interest because of their thermal stabilities and high mechanical strength, and hence there is immense scope for research in this area [15].

A variety of inorganic supports have been employed to immobilize enzyme; the most extensively studied inorganic supports are magnetic nanoparticles [16] and clays such as zeolites, bentonite, and sepiolites [17–19]. Attapulgite (ATP), also known as palygorskite, a kind of hydrated magnesium aluminum silicate containing ribbons of a 2:1 phyllosilicate structure present in nature as a fibrillar silicate clay mineral, has exchangeable cations and reactive $-OH$ groups on its surface [20]. It has the structural formula $Si_8O_{20}Mg_5(Al)(OH)_2(H_2O)_4 \cdot 4H_2O$, and its ideal structure was studied by Bradley early in 1940 and is shown in Fig. 1. The particles are approximately 20 nm in diameter, the length is from several hundred nanometers to several micrometers, and it has high temperature endurance and high surface area [21]. There are large reserves of ATP in South China (Jiang Su, Zhe Jiang, and An Hui provinces) and in the USA (Florida), although ATP has been mainly used as absorbent, catalyst carrier for the applications in various catalytic reactions, densifying agent, adhesive, food additive and a filler, etc [22]. There are no reports about its use in immobilization of ADH up to now.

In this study, a derived ATP was prepared by the covalent binding of 3-aminopropyltriethoxy silane (APTES) onto the surface of ATP, then immobilizing ADH from permeabilized brewer's yeast on the nano-fibrils ATP-APTES via glutaraldehyde coupling reaction. The effect of immobilization on ADH activity, temperature and pH, operational stability, and reusability of immobilized ADH and bioreduction of ethyl 3-oxobutyrate (EOB) to corresponding product (S)-EHB by the immobilized ADH were also investigated in a batch reaction.

Fig. 1 Schematic diagram of ATP

Materials and Methods

Materials

3-Aminopropyltriethoxy silane, 25% glutataldehyde solution, nicotinamide adenine dinucleotide (NAD^+), and ethyl-3-hydroxybutyrate (*R*- and *S*-enantiomers) were purchased from Sigma-Aldrich Chemical Co. Brewer's yeast (*Saccharomyces cerevisiae*) was obtained from Chong Qing Beer Group Ltd., Chongqing, China. The attapulgite nano-fibrillar clay with the average diameter of 325 mesh was supplied by Jiangsu Sinitic Mines Co, Ltd (China). Other chemicals and solvents were obtained from Shanghai Chemical Reagent Co. and were of analytical reagent grade.

Extraction of Alcohol Dehydrogenase from Permeabilized Brewer's Yeast

The extraction of ADH from permeabilized brewer's yeast was performed as described previously with some modifications [23]. Briefly, a typical preparation was as follows: first, fresh brewer's yeast cells were permeabilized with 0.2% w/v cetyltrimethylammonium bromide and harvested by centrifugation at 6,000 rpm at 4 °C for 15 min [1]. Then, disruption of yeast suspension was carried out using ultrasonic vibra cell crusher. The supernatant was collected and precipitated with ammonium sulfate; the precipitant was resuspended and dialyzed after collection. The ADH solution (crude cell extract) was obtained in the supernatant and used for the following experiments.

Derivation and Activation of ATP

For the conventional post-synthesis grafting, APTES was used. The ATP was first added to the aqueous solution of sulfuric acid at 90 °C and stirred overnight. An acid/ATP (w/w) ratio between of 0.2 based on dry weight of ATP and 98% H_2SO_4 was selected to ensure that the layered structure is preserved. The resulting acid-activated ATP were repeatedly washed with deionized water and dried at ambient temperature. Derivation was carried out by adding 1 g of acid-active ATP to 50 ml ethanol/water solution (v/v=75:25) containing 10% APTES. The mixture was refluxed for 5 h with constant stirring. The resulting product was filtered and washed several times with ethanol/water solution to remove excessive

silane coupling agent and dried at 70 °C for 6 h [24]. The derived ATP was treated with glutaraldehyde solution at a ratio of 25 ml solution per gram ATP and magnetically stirred for 3 h at room temperature, filtered, washed, and dried at ambient temperature. The derived ATP containing active carbonyl groups was obtained and used for immobilization of ADH.

Immobilization of ADH

The resulting product (1 g) was mixed with crude ADH solution (5 ml) in 15 ml 0.1 M phosphate buffer solution pH 7.0 and shaken for 2 h in a thermostated water bath shaker at room temperature and then centrifuged at 8,000 rpm at 4 °C for 10 min. The precipitates were washed with 0.1 M phosphate buffer solution pH 7.0 and then directly used for the measurements of activity and stability of ADH.

Enzyme Assay

Enzymatic activity assay of immobilized and free ADH was determined by method of Vallee and Hoch [25] and carried out using 1.5 ml of 0.1 M sodium pyrophosphate buffer (pH 8.8), 0.5 ml of 2 M ethanol, 1 ml of 25 mM NAD⁺ solution, and 50 mg immobilized ADH or 0.1 ml free ADH solution. The absorbance, measured for 5 min at 340 nm, indicated the generation of NADH. One unit of ADH activity is defined as the amount of enzyme required for catalyzing the formation of 1.0 μ mol acetaldehyde from ethanol per minute, at pH 8.8 at 25 °C.

Effect of pH on the Activity of Free and Immobilized ADH

The effect of pH was studied at 25 °C by varying the pH in the range 5.0–9.0. A typical procedure was as follows: 0.1 g immobilized ADH or 1 ml of free ADH solution was mixed with phosphate buffer at different pH from 5.0 to 9.0 and incubated for 30 min at 25 °C. At the end of the incubation time, the activity of both enzymes was analyzed as described above.

Effect of Temperature on the Activity of Immobilized and Free ADH

The optimum temperature was determined by incubating immobilized and free ADH at 0.1 M phosphate buffer pH 7.0 at temperatures in the range 15–50 °C for 30 min. At the end of the time, the enzyme activity of each sample was determined.

pH and Thermal Stability of Immobilized and Free ADH

In order to determine pH stability, 1 ml of free ADH solution or 0.1 g immobilized ADH was mixed with 0.1 M phosphate buffer of different pH (6, 7, and 8) and incubated for 100 min at 25 °C. Samples were withdrawn at different times, and residual activity was measured as previously described. Otherwise, 1 ml of free ADH solution or 0.1 g immobilized ADH were placed in pH 7.0 phosphate buffer and incubated at different temperatures (40–60 °C) for different time intervals. The activity of the enzyme was then determined as described earlier.

Operational Stability of Immobilized ADH

The operational stability of the immobilized ADH was assessed by monitoring their residual activity in 0.1 M phosphate buffer pH 7.0 at optimum temperature for 52 h at

time intervals of 3 h. The activity is represented as percentage of initial activity retained.

Bioreduction of EOB Mediated by Immobilized ADH

The reaction was carried out in a 100-mL Erlenmeyer flask. After 3 g of immobilized ADH was suspended in phosphate buffer (30 mL, pH 7.0) containing 50 $\mu\text{mol NAD}^+$, the reaction was started by continuously feeding into 20 mL of an aqueous solution of 20 mM EOB and 1.2 g of 2-propanol at a rate of 10 drops/min for about 1 h. Flask was incubated at 35 °C for 150 min with continuous shaking at 125 rpm. Every 30 min, 2.0 mL aliquots were taken from the reaction solution and extracted with ethyl acetate. The combined extracts were dried over anhydrous sodium sulfate and filtered. The concentration of product was measured by gas chromatography (GC), as described in “[Analysis of Reactant and Products](#).” The biocatalyst was harvested after reaction, washed with 50 mM phosphate buffer pH 7.0, and used for the next run under the same conditions.

Analysis of Reactant and Products

The concentration and ee value of the product and conversion percentage of substrate were determined by chiral gas chromatography (Agilent GC 6890, Varian Inc., Palo Alto, USA) equipped with a flame ionization detector and a capillary column of cyclosil-B 30 m \times 0.25 mm (i.d., Advanced Separation Technologies Inc., Whippany, NJ, USA). With the flow rate of pure helium 0.7 mL/min, a sample volume of 1 μL was injected using a split ratio of 1:100. Column initial and final temperatures were 85 and 130 °C, respectively. Temperature program was 85 °C for 10 min, 5 °C/min, 90 °C for 15 min, 20 °C/min, 130 °C for 20 min. Retention times for ethyl (S)-3-hydroxybutyrate, ethyl (R)-3-hydroxy butyrate, and ethyl-3-oxobutyrate were 19.53, 20.28, and 16.4 min, respectively.

Results and Discussion

Characterization

ATP was functionalized with organosilane APTES and glutaraldehyde to form a layer of aldehyde groups which react with the amino groups of ADH (Fig. 2). First, ATP was derived by using APTES via a condensation reaction. The ability of organosilanes to bond to surfaces arises from the fact that the ethoxy groups ($-\text{Si}-(\text{OCH}_2\text{CH}_3)_3$) of aminosilanes, such as APTES, form silanols ($-\text{Si}-(\text{OH})_3$) in aqueous solution. These silanol groups can then bond covalently to a suitable substrate, usually inorganic solids displaying appropriate surface chemical groups (such as $-\text{OH}$) [26]. Then, ADH was immobilized to the derived ATP via glutaraldehyde coupling reaction.

Fourier transform infrared (FTIR) spectra using the KBr pressed disk technique were recorded on a Perkin-Elmer Spectrum One FTIR Spectrometer after mixing the samples with KBr in the range from 4,000 to 400 cm^{-1} . Figure 3 displays the FTIR spectra of natural ATP (a), derived ATP (b), and carbonyl-activated ATP-bound ADH (c) samples. The absorption peaks at 3,435, 1,646, and 797 cm^{-1} in the FTIR spectra of natural ATP (a) are due to the $-\text{OH}$ stretching, bending vibrations of the adsorbed water molecules, and $-\text{OH}$ bending vibration of the Mg (Mg) OH group, respectively. For the IR spectrum of derived ATP (b), the peak at 1,080 cm^{-1} is attributed to the Si–O stretching of silicates in

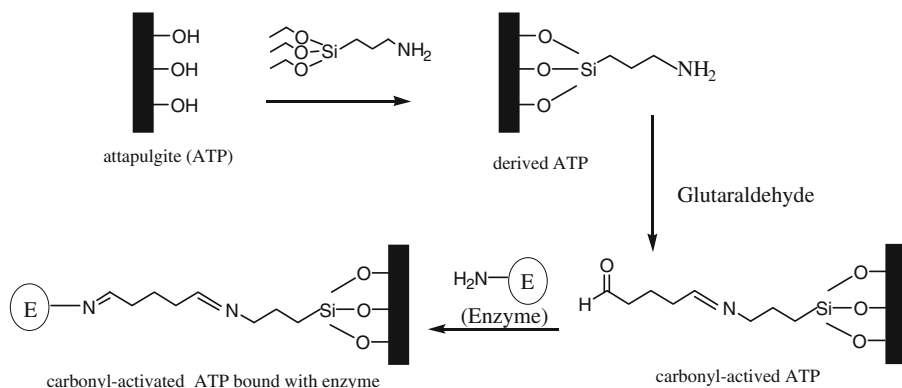


Fig. 2 Illustrations of ATP modification and alcohol dehydrogenase immobilization on the derived ATP

the clay. New peak at $2,940\text{ cm}^{-1}$ is due to the symmetric stretching of $-\text{CH}_2$ groups, and additional peaks at $1,492$ and 698 cm^{-1} correspond to the $-\text{NH}_2$ and $-\text{CH}_2$ bending vibrations, indicating that the $\text{Si}-\text{OH}$ of the natural ATP was grafted with APTES. Compared with the spectrum of derived ATP (b) after binding ADH, new peak appeared at $1,630\text{ cm}^{-1}$ relating to $\text{C}=\text{N}$ group of Schiff base; this peak suggested that the amine group of ADH reacted with the amine group on the derived ATP through glutaraldehyde crosslinking.

Optimization of Glutaraldehyde Concentration

Glutaraldehyde is a bialdehyde functional molecule commonly used as a linker. ADH was immobilized to the derived ATP via the aldehyde function of glutaraldehyde covalent

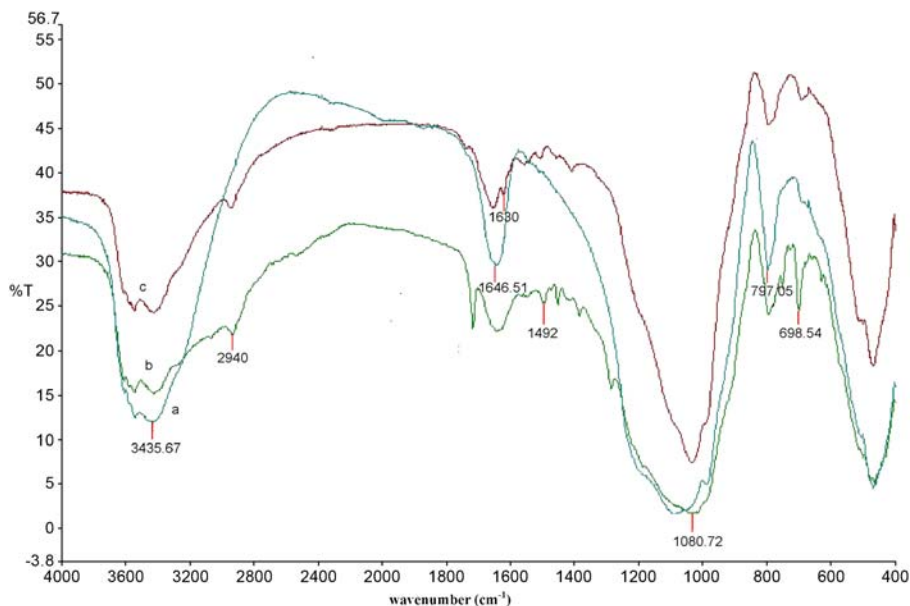


Fig. 3 The FTIR spectra of natural ATP (a), derived ATP (b), and carbonyl-activated ATP bound ADH (c) samples

Table 1 Concentration of glutaraldehyde effect on the activity of immobilized ADH.

Concentration of glutaraldehyde %(v/v)	0.5	1.0	2.5	5.0	10.0
Relativity activity (%)	100	92	84	80	71

Condition: Derived ATP 1.0 g, different concentration of glutaraldehyde solutions 25 ml, stirred for 3 h at room temperature. The obtained carbonyl-activated ATP (1 g), crude ADH solution (5 ml) in 15 ml 0.1 M phosphate buffer solution, pH 7.0, shaken for 2 h in a thermostated water bath shaker at room temperature, and the immobilized ADH were used for the measurements of activity

bonding with amino functional groups of enzyme. The derived ATP was treated with glutaraldehyde solutions of different concentrations ranging between 0.5% and 10%. The results are shown in Table 1. Treating with 0.5% glutaraldehyde solution, the activity of the immobilized ADH is at maximum. It became obvious that with treatment increasing the concentration of glutaraldehyde, the activity of enzyme bound to the ATP support decreases. The decrease in enzyme activity could be the result of a partial denaturation of enzyme by additional bonds between glutaraldehyde and residues of the active center of the enzyme. Another reason for the low activity may be “rigidification” of the enzyme molecule or steric hindrance which prevents the substrate from reaching the active site [27]

Effect of pH

The effect of pH on enzyme activity was studied in the range of 5.0–9.0 at 25 °C. From Fig. 4, the optimum pH for the free and immobilized ADH was 7.0 and 7.5, respectively. The relative activity of the immobilized ADH was always kept higher than the free ADH at various pH. From pH 8.0 to 9.0, both enzymes had significant loss of activity as a result of changes in pH; however, the activity of immobilized enzyme decreases slower than the free ADH. From obtained results, it could be seen that the free ADH is more sensitive to pH than the immobilized ADH, and immobilization method could improve the activity of enzyme especially at higher pH. This was attributed to the charge effects of support and the strong covalent bond formed between the enzyme and the support. Because ATP has permanent negative charges on its surface that may cause partitioning of protons, negatively

Fig. 4 Effect of pH on activity of free and immobilized ADH. Condition: 0.1 g immobilized ADH or 1 ml of free ADH solution in 10 ml phosphate buffer, incubated for 30 min at 25 °C

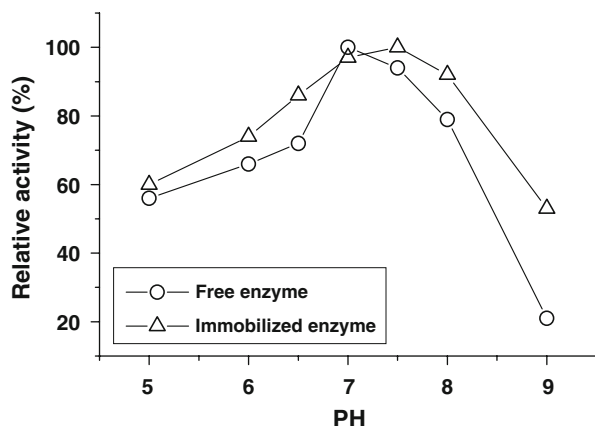
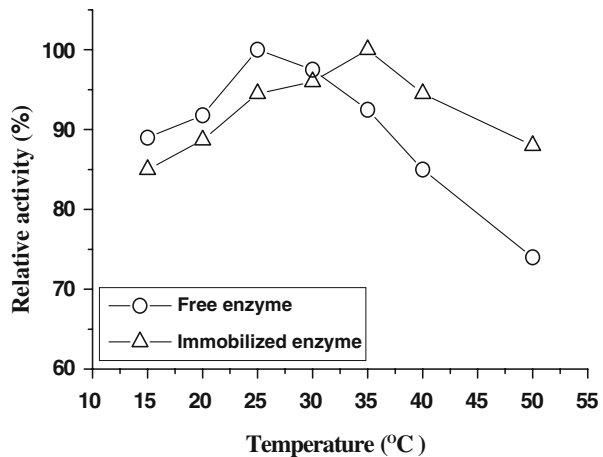


Fig. 5 Effect of temperature on the activity of free and immobilized ADH. Condition: 0.1 g immobilized ADH or 1 ml of free ADH solution, in 10 ml 0.1 M phosphate buffer pH 7.0, incubated for 30 min



charged groups of matrix will tend to concentrate protons (thus lowering the pH) around the enzyme. Therefore, the pH around the enzyme will be lower than that of the bulk phase from which measurement of pH is carried out [28].

Effect of Temperature

The effect of temperature on the activity of free and immobilized ADH was studied in the range from 15 to 50 °C. The optimum temperature of the free ADH was at 25 °C, whereas the immobilized ADH showed highest activity at 35 °C (Fig. 5). The results show that a further increase in temperature led to a gradual decrease in the remaining activity of both free and immobilized enzymes. At higher temperatures, the activity of both forms of enzymes decreased due to thermal inactivation of the enzyme, but the immobilized ADH kept higher relative activity than the free ADH. From the results, it is found that the immobilized ADH could lower the rate of inactivation of enzyme and be less sensitive to the change of temperature compared to the free ADH. Since in the bound state enzymes are less mobile, therefore, it could resist denaturation of enzyme by the influence of temperature.

pH and Thermal Stability of Immobilized and Free ADH

pH stability was investigated by incubating immobilized and free ADH at pH value ranging from 6.0 to 8.0 in 0.1 M phosphate buffer for 100 min. Figure 6a, b shows the loss of the enzyme activity incubated for different lengths of time at various pH. The immobilized ADH demonstrated greater stability than the free form (Fig. 6). At pH 6.0 and 8.0, the activity of free ADH decreased dramatically during the incubation, and 90 min later, most of the activity was lost. However, the immobilized form retained 81% of activity at pH 8.0. This indicates that immobilization brought about enhanced pH stability and retention of inactivation from changing pH increases upon immobilization.

Thermal stability of immobilized and free ADH was determined by incubating them in phosphate buffer at 40, 50, and 60 °C in different times. Residual activity of enzyme was calculated with respect to its initial activity. Figure 7a, b shows a comparison of free and immobilized ADH. It was observed that the enzyme activity decreased with the temperature

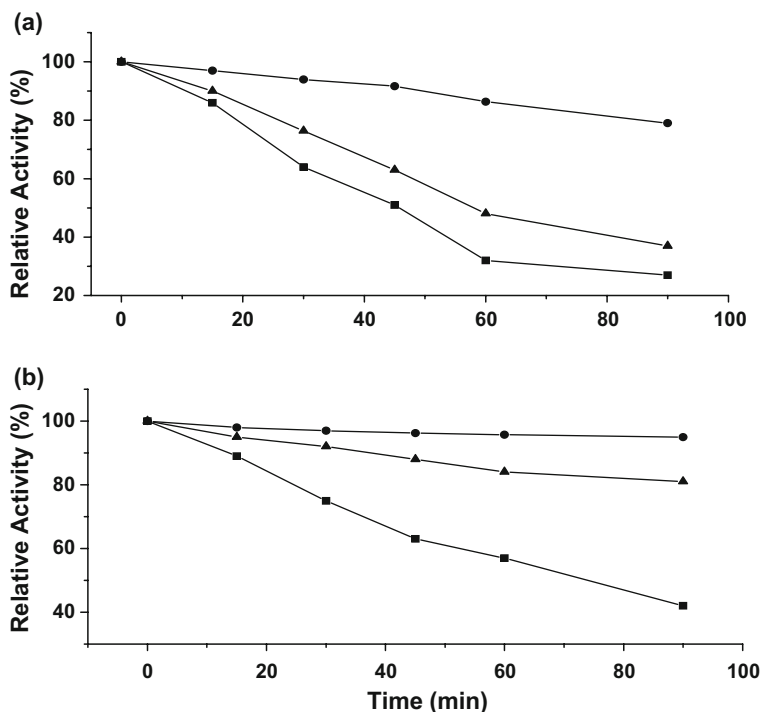


Fig. 6 pH stability of **a** free ADH and **b** immobilized ADH incubated for 100 min in pH 6.0, 7.0, and 8.0 phosphate buffer at 25 °C

for both free and immobilized ADH. However, the immobilized ADH has a higher thermal stability than that of the free. Free enzyme loses its 68% activity, whereas immobilized ADH retained 44% over a 60-min incubation at 60 °C. These indicated the improved thermal stability of immobilized system than free ADH.

Operational Stability of Immobilized ADH

Operational stability of the immobilized ADH was determined by measuring the enzyme activity periodically with continuous shaking at 125 rpm at 35 °C. The results in Fig. 8 showed that the catalytic activity that remained did not obviously change for 15 h period. When the operation time increased, immobilized ADH activity decreased gradually. After shaking for 32 h, a rapid loss in activity was observed, and almost complete activity of enzyme was lost in 52 h. These results could be explained by the inactivation of the enzyme caused by the denaturation of the protein and the leakage of protein from the support upon long-term usage.

Bioreduction

In the bioreduction process with substrate-coupled cofactor regeneration, 2-propanol was used as cosubstrate. The time dependence of the bioreduction was demonstrated with samples taken at short time intervals (every 30 min). Figure 9 shows that when 20 mM EOB was continuously added at a rate of 10 drops/min for about 1 h to a suspension

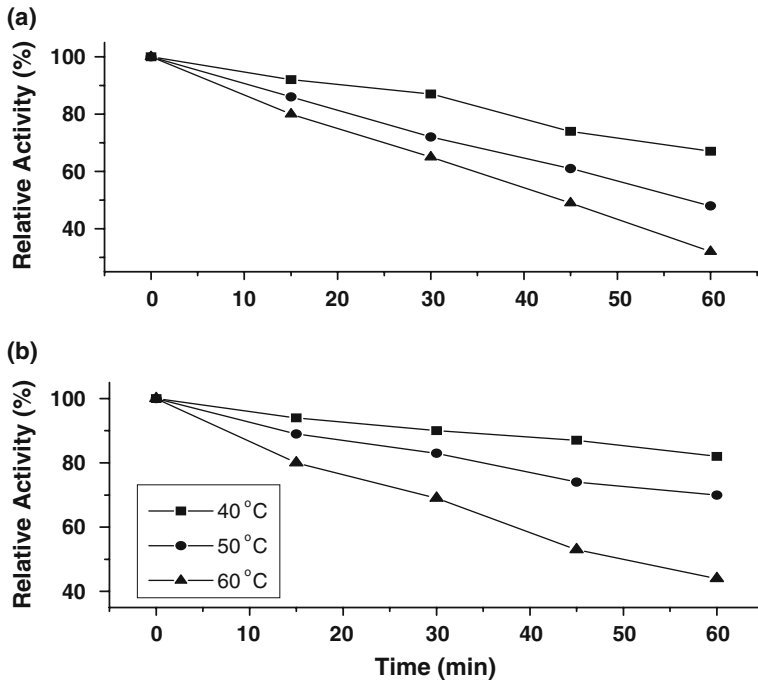


Fig. 7 Thermal stability of **a** free ADH and **b** immobilized ADH incubated for 60 min in pH 7.0 phosphate buffer at different temperatures (40, 50, and 60 °C)

containing 3 g immobilized ADH, initial 120 min was the most important period for bioreduction; the product (*S*)-EHB concentration increased up to 17.6 mM within 120 min accompanied by the conversion of EOB up to 88%, and the ee value reached in excess of 99%. After this, the concentration of substrate and product did not obviously change. Therefore, the reaction system has reached equilibrium at 120 min in this case. The results suggested that the immobilized ADH can efficiently perform bioreduction of EOB to the

Fig. 8 Operational stability of immobilized ADH in 0.1 M pH 7.0 phosphate buffer solution at 35 °C shaking at 125 rpm for 52 h

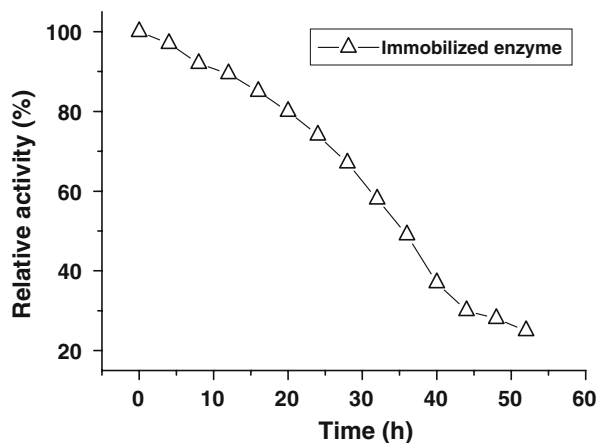
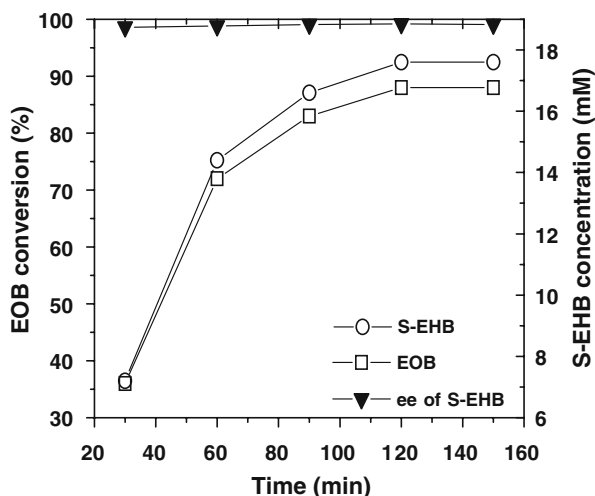


Fig. 9 Reaction time-course for the reduction of ethyl 3-oxobuturate into ethyl(*S*)-3-hydroxy buturate catalyzed by the immobilized ADH. Reaction condition: 20 mM EOB, 1.2 g of 2-propanol, 50 μ mol NAD^+ , 0.06 g/ml immobilized ADH, 50 ml 0.1 M phosphate buffer (pH 7.0)

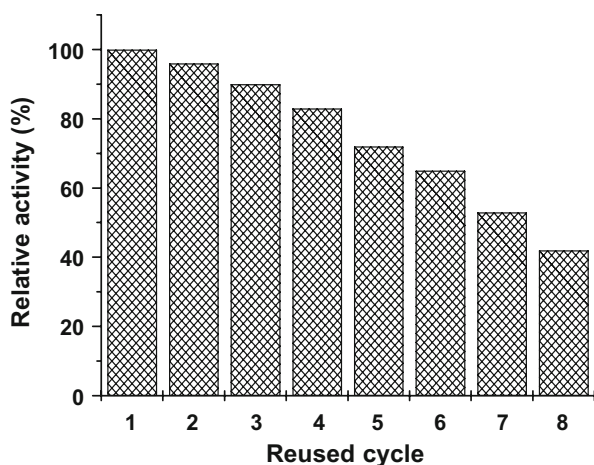


corresponding (*S*)-alcohols which are a promising chiral building block for the chemical synthesis of antibiotics, pheromones, and more complex chiral intermediates [29].

Reuse of Biocatalyst

The reusability of immobilized ADH was examined by measuring the activity of the biocatalyst after each cycle. Relative activity of the immobilized enzyme at repeated use is shown in Fig. 10. The relative activity of the immobilized enzyme compared to its initial value in percentage decreased along with the reusing times. As shown in Fig. 10, the activity of immobilized ADH decreased to 80% of its initial value after four cycles of operation and afterwards gradually decreased with every reuse, but it retained 42% activity after eight cycles for bioreduction of EOB to S-EHB.

Fig. 10 Relative activity of immobilized ADH after repeated use for bioreduction of EOB to S-EHB



Conclusions

An attractive feature of extraction and immobilization of the ADH from permeabilized brewer's yeast on the derived ATP via glutaraldehyde coupling reaction is that it is readily available and very easy to handle. More importantly, the immobilized ADH not only exhibited good operational stability and reusability but also could successfully be employed for the bioreduction of EOB to (*S*)-EHB with high optical purity ($\geq 99\%$). Moreover, Jülich Fine Chemicals and Wacker Specialties (JFC-Wacker) collaboration develops and uses ADHs as biocatalysts. An important example of an ADH is from *Rhodococcus erythropolis* (ADH RE), which leads to (*S*)-configured 3-hydroxyesters. Any of the methyl, ethyl, and tert-butyl esters of 3-oxobutyrate gives complete reduction to the corresponding enantiopure ($ee > 99\%$) [5, 29]. The combination of these means that the ADH (crude cell extract) from permeabilized brewer's yeast immobilized on the derived ATP via glutaraldehyde covalent binding would probably be a more promising biocatalyst for the production of (*S*)-configured chiral alcohols.

Acknowledgments This work was supported by the special fund of three items of expenditure on Science and Technology Department of Central District in ChongQing. We also thank the Chongqing Medical University for partial financial support of this work.

References

1. Yu, M. A., Wei, Y. M., Zhao, L., Jiang, L., Zhu, X. B., & Qi, W. (2007). *J Ind Microbiol Biotechnol*, 34, 151–156. doi:10.1007/s10295-006-0179-z.
2. Yu, M. A., Hou, Y., Gong, G. H., Zhao, Q., Zhu, X. B., Jiang, L., et al. (2009). *J Ind Microbiol Biotechnol*, 36, 157–162. doi:10.1007/s10295-008-0483-x.
3. Zhang, J., Witholt, B., & Li, Z. (2006). *Chem Commun*, 4, 39–400. doi:10.1039/b515721h.
4. Zhang, J., Witholt, B., & Li, Z. (2006). *Adv Synth Catal*, 348, 429–433. doi:10.1002/adsc.200505439.
5. Daußmann, T., Rosen, T. C., & Dünkelfmann, P. (2006). *Eng Life Sci*, 6, 125–129. doi:10.1002/elsc.200620910.
6. Sheldon, R. A. (2007). *Adv Synth Catal*, 349, 1289–1307. doi:10.1002/adsc.200700082.
7. Erdemir, S., & Yilmaz, M. (2008). *J Mol Catal B: Enzym*, . doi:10.1016/j.molcatb.2008.11.008.
8. Temiño, D. M., Hartmeier, W., & Ansorge-Schumacher, M. B. (2005). *Enzyme Microb Technol*, 36, 3–9. doi:10.1016/j.enzmctec.2004.01.013.
9. Goldberg, K., Krueger, A., Meinhardt, T., Kroutil, W., Mautner, B., & Liese, A. (2008). *Tetrahedron Asymmetry*, 19, 1171–1173. doi:10.1016/j.tetasy.2008.04.034.
10. Bolivar, J. M., Wilson, L., Ferrarotti, S. A., Guisán, J. M., Fernández-Lafuente, R., & Mateo, C. (2006). *J Biotechnol*, 125, 85–94. doi:10.1016/j.jbiotec.2006.01.028.
11. Katchalski-Katzir, E., & Kraemer, D. M. (2000). *J Mol Catal B: Enzym*, 10, 157–176. doi:S1381-1177-00.00124-7.
12. Zhang, L., Jiang, Y. J., Shi, J. F., Sun, X. H., Li, J., & Jiang, Z. Y. (2008). *Reactive and Functional Polymers*, 68, 1507–1515. doi:10.1016/j.reactfunctpolym.2008.08.007.
13. Soni, S., Desai, J. D., & Devi, S. (2001). *J Appl Polym Sci*, 82, 1299–1305.
14. Sinegani, A. A. S., Emtiazi, G., & Shariatmadari, H. (2005). *J Colloid Interface Sci*, 290, 39–44. doi:10.1016/j.jcis.2005.04.030.
15. Sanjay, G., & Sugunan, S. (2008). *J Porous Mater*, 15, 359–367. doi:10.1007/s10934-006-9089-8.
16. Liao, M. H., & Chen, D. W. (2001). *Biotechnological Letters*, 32, 1723–1727.
17. Seetharam, G., & Saville, B. A. (2002). *Enzyme Microb Technol*, 31, 747–753. doi:S0141-0229(02)00182-5.
18. Yeşim, Yeşiloğlu. (2005). *Process Biochem*, 40, 2155–2159. doi:10.1016/j.procbio.2004.08.008.
19. Prodanovic, R. M., Simic, M. B., & Vujcic, Z. M. (2003). *J Serb Chem Soc*, 68, 819–824. udc: 542.943+664. 164:541. 183+ 679.91+547.458.2.

20. Zhang, J. P., Wang, Q., & Wang, A. (2007). *Carbohydrate Polymers*, 68, 367–374. doi:[10.1016/j.carbpol.2006.11.018](https://doi.org/10.1016/j.carbpol.2006.11.018).
21. Liu, Y. S., Liu, P., & Su, Z. X. (2008). *J Appl Polym Sci*, 107, 2082–2088. doi:[10.1002/app.27358](https://doi.org/10.1002/app.27358).
22. Tian, M., Qu, C. D., Feng, Y. X., & Zhang, L. Q. (2003). *J Mater Sci*, 38, 4917–4924.
23. Li, G. Y., Huang, K. L., Jiang, Y. R., Yang, D. L., & Ding, P. (2008). *International Journal of Biological Macromolecules*, 42, 405–412. doi:[10.1016/j.ijbiomac.2008.01.005](https://doi.org/10.1016/j.ijbiomac.2008.01.005).
24. He, H. P., Duchet, J., Galy, J., & Gerard, J. F. (2005). *J Colloid Interface Sci*, 288, 171–176. doi:[10.1016/j.jcis.2005.02.092](https://doi.org/10.1016/j.jcis.2005.02.092).
25. Vallee, B. L., & Hoch, F. L. (1955). *Proc Nat Acad Sci*, 41, 327–338.
26. Siperko, L. M., Jacquet, R., & Landis, W. J. (2006). *J Biomed Mater Res*, 78A, 808–822. doi:[10.1002/jbm.a.30731](https://doi.org/10.1002/jbm.a.30731).
27. Marty, J. L. (1985). *Applied Microbiology and Biotechnology*, 22, 88–91.
28. Erginer, R., Toppare, L., Alkan, S., & Bakir, U. (2000). *React Funct Polym*, 45, 227–233. doi:[S1381-5148\(00\)00036-5](https://doi.org/10.1016/S1381-5148(00)00036-5).
29. Rosen, T. C., Daussmann, T., & Stohrer, J. (2004). *Speciality Chem Mag*, 24, 39–40.